한국지반공학회논문집 제26권 4호 2010년 4월 pp. 15 ~ 26

Frost-Heaving Characteristics of Soil Mixed with Discarded Tire Powder

폐타이어 파우더 혼합토의 동상 특성

Kim, Hak-Sam[1] 김 학 삼
Suh, Sang-Youl[2] 서 상 열
Nakamura, Dai[3] 中村 大
Fukuda, Masami[4] 福田 正己
Yamashita, Satoshi[5] 山下 聡
Suzuki, Teruyuki[6] 鈴木 輝之

요 지

폐타이어 파우더 혼합에 따른 동상억제 메커니즘을 규명하기 위해, 부동수, 열전도율, 동상실험 등 3종류의 실내실험을 수행하였다. 본 연구에서는 폐타이어 혼합에 따른 투수계수 변화에 주목하여 먼저 미동결토의 불포화 투수계수를 계산하였고 ice-impeding factor, 혼합토내 토립자와 폐타이어 단면적을 고려하여 동결토frozen fringe내의 온도변화에 따른 투수계수 특성을 분석하였다. 그 결과 흡수속도와 투수계수 사이에는 비례관계가 존재함을 확인하였고, 동상성 저하의 주된 원인은 폐타이어 파우더 혼합에 따른 부동수분량과 투수계수의 감소임을 알 수 있었다. 또한 폐타이어 파우더 혼합토 구성성분의 체적비를 이용하여 흙과 폐타이어 간극내의 수분량을 정량적으로 산출하였다.

Abstract

To determine the frost heave suppressing mechanism of soil mixed with tire powder, we conducted three kinds of laboratory experiments: measurement of unfrozen water, evaluation of thermal conductivity, and a frost heave. In this research, we focused on changes in the coefficient of permeability of the mixed soil, and first found that of the unsaturated soil. Next, in the case of the presence of ice, we took the ice-impeding factor into consideration to derive the coefficient of permeability of the frozen fringe from the area ratio of the soil and tire powder in mixed soil. The results show a positive correlation between the water intake rate and the coefficient of permeability. Moreover, we found that the frost heave decreased thanks to a reduction in the permeability and a fall in the unfrozen water content of the soil mixed with tire powder. We also calculated the weight of the water content of the soil and tire powder void quantitatively using the result of the volumetric ratio of mixed soil.

Keywords : Discarded tire, Frost heave, Permeability, Thermal conductivity, Unfrozen water content

1. Introduction

As cars are increasing in production and becoming popular, the number of discarded tires is rising. In 2008, the nationwide amount reached 16,000,000 tires (300,000 tons in weight). Although used tires are designated as

1 Associate Prof., Dept. of Civil Engrg., Yeungnam College of Science & Technology, kimhs@ync.ac.kr, 교신저자
2 Member, Prof., Dept. of Civil Engrg., Yeungnam College of Science & Technology
3 Assistant Prof., Dept. of Civil and Environmental Engrg., Kitami Institute of Technology
4 Visiting Prof., International Arctic Research Center, Univ. of Alaska
5 Prof., Dept. of Civil and Environmental Engrg., Kitami Institute of Technology
6 Prof., Dept. of Civil and Environmental Engrg., Kitami Institute of Technology
* 본 논문에 대한 토의를 원하는 회원은 2010년 10월 31일까지 그 내용을 학회로 보내주시기 바랍니다. 저자의 검토 내용과 함께 논문집에 게재하여 드립니다.

industrial waste, users sometimes dispose of them illegally without correct handling or recycling, which result in environmental degradation. In order to address this environmental problem and to increase the recycling rate of waste tires as part of efforts to reuse valuable waste, the development and research of various technologies are urgent tasks. Korea now recycles discarded tires by using them mainly as fuel at power plants, cement material, regenerated tire and has tried to take advantage of them as a civil engineering material to raise the recycling rate further. In the U.S., waste tires used as a civil engineering material account for about 13% of total volume, and this number is rising. The cold regions of Russia suffer from the frost heave of roads and buildings, and costs for repairs are becoming significant. As reported by Eaton et al. (1994), Zimmer (1996), and Humphrey et al. (1997), some attempts have been made as measures against damage caused by frost heave; for example, discarded tires are buried in road bases or beds. The spotlight now centers on these uses as a method of using waste tires aggressively.

The combination of the recycling of discarded tires and action against frost heave is an unprecedented application, but sufficient verification of the effectiveness has not yet been made. Conventionally, the replacement method was employed as one measure against the frost heave of roads when frost heave is anticipated in the existing materials; the road base or bed is replaced with a frost heave resistant material. According to Ifukube (1962), the replacement depth should be 70 percent of the maximum freezing depth of a place. Accordingly, the actual consumption of sand or gravel used as the frost-heave-resistant replacement material is very high. In addition, regional development makes it more difficult to obtain high-quality materials and increases road construction costs. Against this background, attention is paid to the development of new granular materials and to the technological development of producing a frost heave resistant material by mixing local soil with an appropriate granular material.

The above means that if waste tire powder could be used as a frost heave resistant material in place of sand or gravel, two effects would be expected: the recycling of the waste resources and the development of a new frost heave suppressing material. Humphery et al. (1997) reported the feasibility of using waste tires featuring low thermal conductivity as a material suppressing the frost heave of roads through a field test in which tire chips (up to 10 cm square) were laid under the ground to a certain thickness. The test results showed that the rubber reduced the freezing depth thanks to its heat insulation effect, but here a serious problem was pointed out, that is the tire chip was easier to compress than soil, resulting in a high risk of destroying the road surface.

In this research, we mixed soil with discarded tire powder that has lower compressibility compared to tire chips to construct soils, and measured the rate of frost heave and SP (Segregation Potential) value in three seasons from 1996 to 1999. Through these measurements, we confirmed the frost heave suppressing effect of the discarded tire powder (Kim et al., 2010).

In parallel with the field experiment described above, we conducted a laboratory experiment to check the relationship between the mixing ratio of discarded tire powder and the resulting frost heave. Specifically, we conducted a ramping frost heave experiment where the freezing speed kept constant to prevent the boundary conditions from varying depending on the unfrozen water content, thermal conductivity, and sample length.

2. Characteristics of Soil and Discarded Tire Powder Samples

Samples used for the frost heave experiment were soil collected in the vicinity of Tomakomai City, Hokkaido Japan. The collected soil contained a large amount of sand with large grain size and its specific surface area covered as large as 54 m^2/g (Kinosita, 1979). We utilized liquid nitrogen (LN_2) to freeze discarded tires at -120 degrees Celsius for 15 minute, and then used a crusher to pulverize them. Subsequently, we used a strong magnet to remove metals from the powder, and passed the powder through a sieve to use only powder having a grain size of 1 mm or less - - nearly equivalent to particle size of a sand. In this test, we made four kinds of samples having different soil contents (in weight): 100% soil, 95% soil + 5% powder,

Table 1. Basic physical properties of each sample

Soil + Tire powder	S100%	S95%+TP5%	S70%+TP30%	S40%+TP60%	TP100%
Dry density (g/cm^3)	1.79	1.71	1.36	1.29	–
Permeability (cm/sec)	4.03×10^{-6}	6.93×10^{-6}	9.45×10^{-6}	1.15×10^{-5}	–
Specific gravity	2.66	2.49	1.97	1.55	1.12

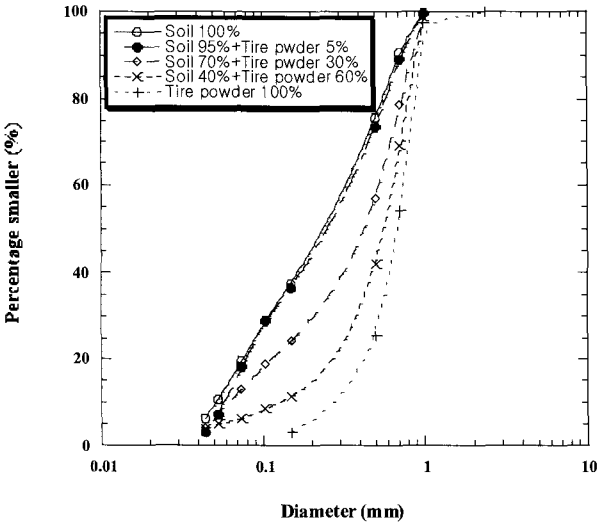

Fig. 1. Particle size distribution curve of each sample

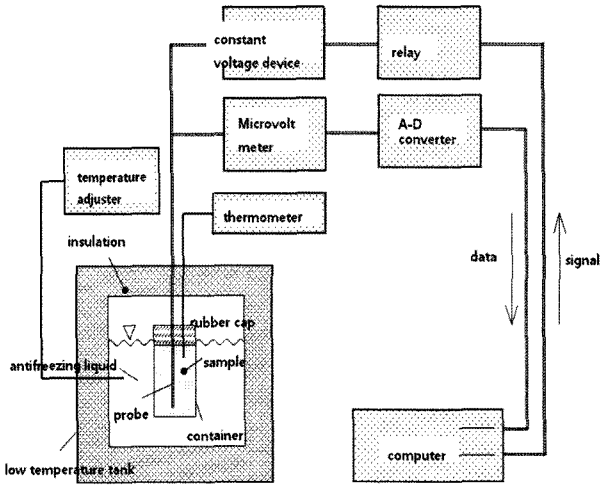

Fig. 2. Schematic diagram of the thermal conductivity equipment

70% soil + 30% powder, and 40% soil + 60% powder. Fig. 1 shows the particle size distribution of each sample, and Table 1 indicates the results of a physical test.

3. Outline of the Experiment

3.1 Measuring the Unfrozen Water Content

We used the pulsed nuclear magnetic resonance (NMR) method to measure the unfrozen water content in frozen soil. Before the experiment, we dried the samples at 110 degrees Celsius, added distilled water until the water content reached a given value, and filled tubes with each sample so that the dry density was 1 g/cm^3 and the volume was 20 cm^3. We turned off the pulse output after the magnetization direction of the sample was set to 90 degrees to allow the direction to return to the original equilibrium. We used a detection coil to measure changes in the magnetizing state. The amplitude of the NMR's FID (Free Induction Decay) signal varies depending on the number of protons in ice and unfrozen water. Since the FID signal of ice drops very quickly, the detected signal is proportional to the number of protons in unfrozen water. Therefore, we found the unfrozen water content from the peak value of the FID signal (Ishizaki, 1994).

3.2 Measuring Thermal Conductivity

To measure thermal conductivity, we employed a thermal probe method (Fig. 2), one of the transient heat flow methods. Before the experiment, we filled a cylindrical plastic container (12 cm in outer diameter and 15 cm in height) with the sample soil at a given density, vertically inserted the probe in the center of the upper part of the sample, and put a rubber stopper to the container in order to prevent the sample from drying and to minimize the influence of heat flow from above. Next, we immersed the container in a thermostatic bath whose temperature was set at -20 degrees Celsius. We changed the temperature from -20 degrees to -15, -10, -5, -2, +5, and +10 degrees in a stepwise manner, and after the sample temperature was kept constant, we measured the thermal conductivity (one step a day).

3.3 Frost Heave Experiment

3.3.1 Experimental Apparatus

The schematic diagram of one dimensional frost heaving apparatus is given in Fig. 3. We filled an acrylic cylindrical cell measuring 10 cm in inner diameter, 1 cm in thickness, and 15 cm in height with each sample. The apparatus was placed in a low-temperature thermostatic chamber whose temperature was set at 4 ± 2 degrees Celsius. We arranged thermo-modules on the upper and lower ends of the cell to control the temperatures of both ends of the sample. In addition, we measured the plate temperatures during testing with platinum resistance temperature sensors (precision: 0.01 degrees Celsius) inserted into the upper and lower plates. We also measured changes in the temperature of each sample with seven thermocouples (precision: 0.1 degrees Celsius) that were embedded in the cell wall and that were aligned 1 cm apart from each other. To reduce the friction between the sample and cell container during testing, we applied silicon oil to the inner wall of the cell. Moreover, to minimize a frictional effect produced by the frozen sample adhering to the frozen cell, we frozed the soil from bottom to top, and supplied water from the top with a burette. To create a one-dimensional heat flow in the sample during testing, we wound 5-cm-thick sponge around the acrylic cell to cut off heat flow in the radial direction.

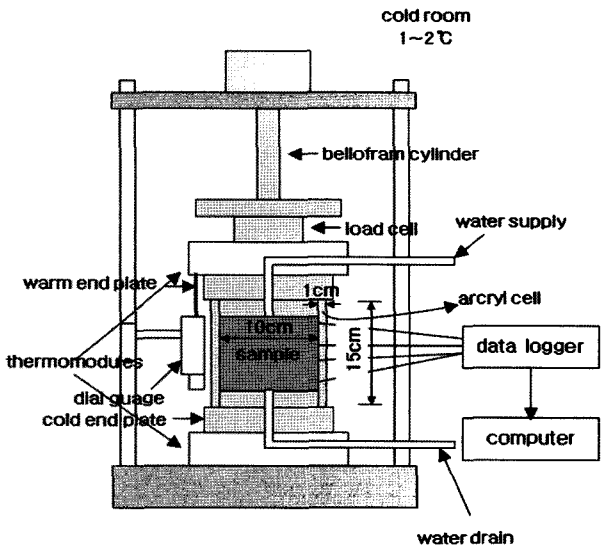

Fig. 3. Frost heave apparatus

3.3.2 Experiment Method

We frozed each sample from the bottom by the ramped freezing method featuring a constant difference between the two end temperatures and a constant temperature gradient. After adding water to the dry sample until the water content became 70 percent, we kept it in a vacuum pump for 24 hours for perfect saturation. We filled the cell with the sample, gradually pressurized it at from 20 kPa up to 100 kPa, and then reduced the pressure to 25 kPa for expansion. The initial state of the sample was completed when the expansion ended. During measurement, we took advantage of hydrostatic pressure to supply water from the lower plate and discharge it from the upper plate, and found the coefficient of permeability of each mixed soil in the cell. After that, we started a frost heave experiment. To first stop the supercooling of pore water in the soil, we cooled down the lower plate at less than -5 degrees Celsius for a short time to form ice cores. After confirming the formation of ice, we set an initial temperature to both ends of the sample and started the experiment. Every hour, we measured the amount of frost heave, the amount of heave by water, and temperatures at both ends. After the experiment ended, to check changes in the water content distribution of the sample, we sliced it into pieces 1 cm thick to measure the water content. Table 2 shows the conditions of this experiment. For example, "3-0.042t" of the notations shown in the table indicates that the initial temperature is 3 degrees Celsius and then it reduces at a rate of 0.042 degrees per hour.

4. Experiment Results

4.1 Unfrozen Water Content

Unfrozen water content is typically represented as the

Table 2. Experiment conditions

Test type	Ramped freezing
Overburden pressure	25kPa
Temperature of upper plate	3℃−0.042t
Temperature of lower plate	0℃−0.042t
Temperature gradient	0.4℃/cm
Experiment duration	72hr.

volumetric ratio (%) of unfrozen water existing in a unit volume of soil. Fig. 4 shows variations in the unfrozen water content of soil mixed with discarded tire powder, which we measured with the pulsation NMR system while varying the temperature. The unfrozen water content reduces sharply when the temperature decreases from zero to -3 degrees, but the gradient is gentle at temperatures of -5 degrees or less. From the resulting curves shown in Fig. 4, we represent the relationship between the unfrozen water content and temperature as a power function of temperature as shown in Eq. (1), where a and b are the factors of each sample given by the least-squares method of measured values, and r is the resulting coefficient of correlation, which are indicated in Table 3. The curves represent the unfrozen water content θ_u derived from these constants.

$$\theta_u = a \cdot |T|^b \qquad (1)$$

where, θ_u is the unfrozen water content (%), T is the absolute value of the mixed soil temperature (℃), and a and b are constants.

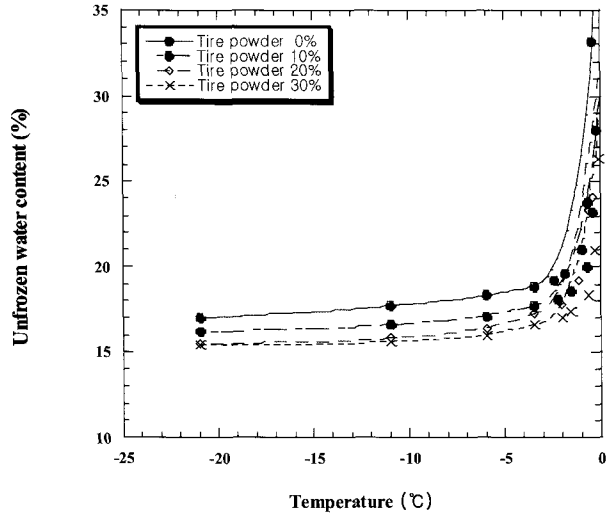

Fig. 4. Variations of unfrozen water content by temperature

Table 3. Factors a and b, and correlation coefficient r for unfrozen water content θ_u

Factors (a, b) Coefficient (r)	a	b	r
0	23.408	−0.136	0.844
10	20.825	−0.107	0.923
20	20.620	−0.115	0.949
30	18.966	−0.092	0.932

As shown in Table 2, the four kinds of soil used in this experiment have values of correlation coefficient r ranging from 0.844 to 0.949 when the relationship between temperature and unfrozen water content is represented by Eq. (1). This means that the relationship between the temperature T and the unfrozen water content θ_u can be represented by Eq. (1).

Fig. 4 shows that as the mixing ratio of discarded tire powder increases, the unfrozen water content tends to decrease. We think that this phenomenon is caused mainly by a reduction in the unfrozen water content of the mixed soil per unit volume. This is because the waste tire powder is rubber that cannot form absorbed water, which may be unfrozen, on the surface of powder particles. Accordingly, we believe that the unfrozen water content of the mixed soil per unit volume is inversely proportional to the powder mixing ratio.

4.2 Thermal Conductivity

Fig. 5 indicates variations in the thermal conductivity λ with the mixing ratio of waste tire powder parameterized when the sample temperature changes from -20 to +10 degrees Celsius. The thermal conductivity rises slightly with increasing sample temperature - - it is almost constant in the unfrozen area at temperatures above zero. However,

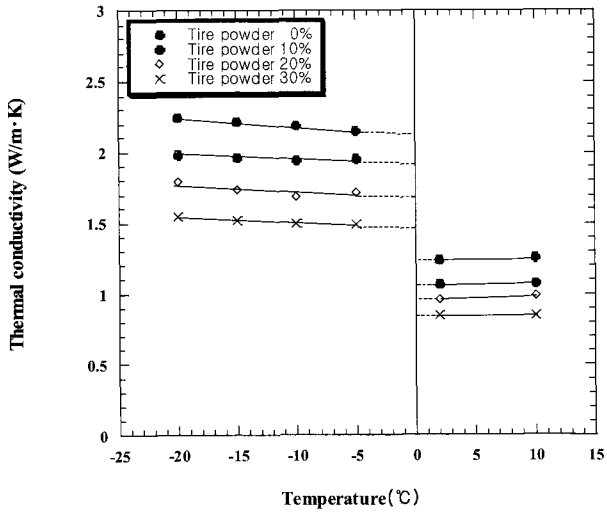

Fig. 5. Relationship among mixing ratio, temperature, and thermal conductivity

thermal conductivity increases significantly when the temperature falls below zero and water contained in the sample is frozen. This is because freezing at zero changes the thermal conductivity from that of water (0.6 W/m·K) to that of ice (2.3 W/m·K). As the temperature decreases, the thermal conductivity increases gradually. As shown in Fig. 4, these changes reflect a phase change phenomenon in which unfrozen water is gradually changing to ice.

According to Fig. 5, when the temperature changes from -5 to -20 degrees, the thermal conductivity of each sample increases by about 0.04 to 0.08 W/m·K. We think that such a rise is caused by the unfrozen water content of frozen soil.

4.3 Frost Heave Experiment

Fig. 6 presents an example of variations in amount of the frost heave and the heave by water over elapsed time. Where, the latter is given by dividing the volume of water intake (cm^3) by the cross section (cm^2) of the sample. The frost heave and the heave by water are represented as a straight line, which accurately reproduces a phenomenon in which the soil shows a frost heave accompanying water intake. In addition, the figure shows that the frost heave is slightly larger than the heave by water. This difference is caused by the fact that when absorbed pore water changes to ice on the ice lens growing surface, the volume expands by nine percent. In this experiment, as shown in Fig. 7, we reduced the temperatures T_C and T_W of the upper and lower ends at a constant rate while keeping the difference between the two constant. As a result, the freezing front moved at a constant speed. Fig. 7 also shows that when the temperature T_W of the upper end falls below zero 72 hours after the start of the experiment, the frost heave stops growing, because pore water in the supply pipe in the upper plate is frozen, resulting in a stop of water supply. Therefore, we ended the experiment at that point.

Fig. 8 shows the relationship between the amount

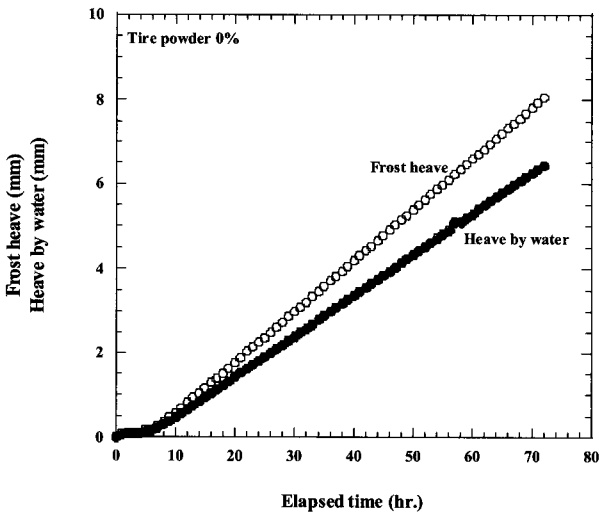

Fig. 6. Variations in amount of frost heave and heave by water

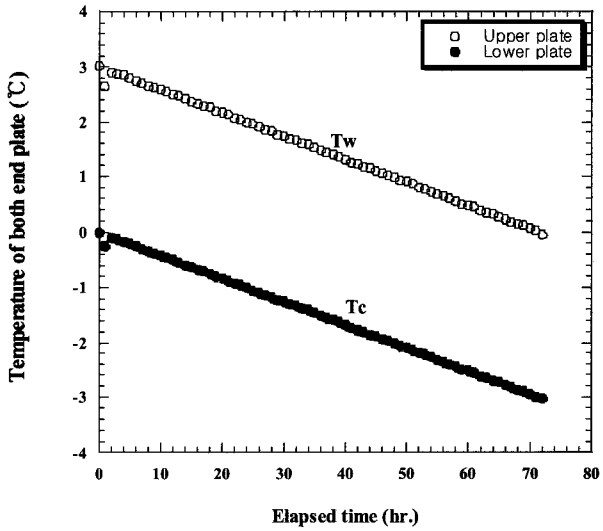

Fig. 7. Variations in end temperatures T_W and T_C over elapsed time

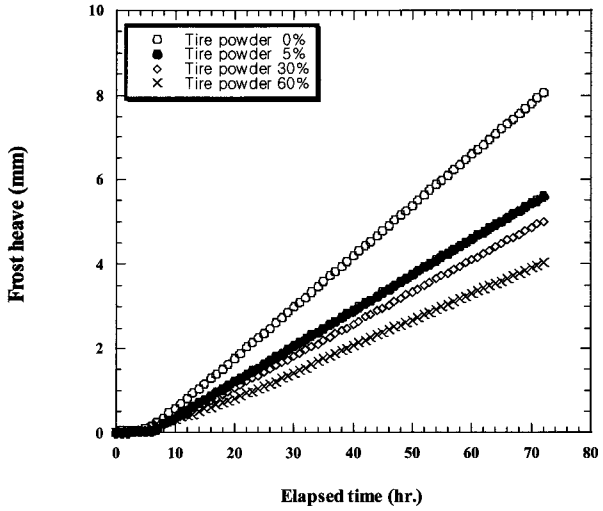

Fig. 8. Variations in frost heave mixed with tire powder over elapsed time

of frost heave and time when Tomakomai soil is mixed with discarded tire powder. The amount of frost heave increases linearly over time except in the initial stage of the experiment. The higher the mixing ratio of tire powder, that has non-frost heaving characteristics, the smaller the amount of frost heave, resulting in a reduction in the rate of frost heave.

Fig. 9 shows results from cutting the extracted sample into pieces 1 cm thick after the frost heave experiment, and measuring the water content on a layer basis. Frozen soil includes soil grains, unfrozen water, and ice, but the last two contents cannot be identified separately. Accordingly, we regard the ice as the water and find the total amount of water. As shown in Fig. 9, we found no common tendency in the water content distribution with respect to the sample height direction. However, as the mixing ratio of tire powder contained in the mixed soil increases, the moisture ratio of the sample decreases.

5. Consideration

5.1 Volumetric Ratio of Voids in the Soil and Tire Powder

To investigate the effect of mixing of discarded tires on the suppression of a frost heave, we must know the volume of water in void of two kinds of grains (soil and waste tire powder) having different physical properties. First, we can derive V_S (volume of the soil in the sample), V_T (volume of the tire in the sample), V_W (volume of the water), W_S (weight of the soil in the sample), and W_T (weight of the tire in the sample) from the three phases of the soil by using the post-test physical properties of each mixed soil listed in Table 1. Table 4 shows the resulting values.

Fig. 10 is a schematic diagram showing the cross-sectional states of the non-mixed and mixed soils. Assuming that the dry density of the soil component in both samples is constant regardless of the mixing ratio of tire powder in the figure, we use the following equation to find the volume of water in the soil and tire powder voids while increasing the mixing ratio. Fig. 10 (a) suggests that V_{SW} (volume of pore water in the soil void) and V_{TW} (volume of pore water in the tire powder void) can be given by the following equations:

$$V_{SW} = V_{S+V} - V_S \tag{2}$$

$$V_{TW} = V_W - V_{SW} \tag{3}$$

where, V_{S+V} is the total volume of the soil component. Table 5 lists the volume of pore water in the soil and tire powder that is derived from Eqs. (2) and (3).

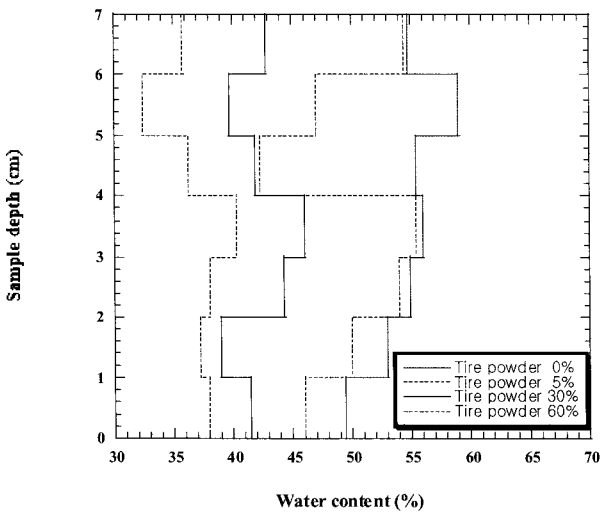

Fig. 9. Water content distribution after experiment

Table 4. Volume and weight of each sample

Mixing ratio (%)	0	5	30	60	
Vs (cm^3)	256.8	245.1	205.1	199.8	
Vw (cm^3)	332.0	316.9	257.0	201.3	V = 588.8 cm^3
V_T (cm^3)	0	26.8	126.7	187.6	
Ws (g)	683.0	604.9	506.6	375.4	
W_T (g)	0	32.2	152.1	225.2	

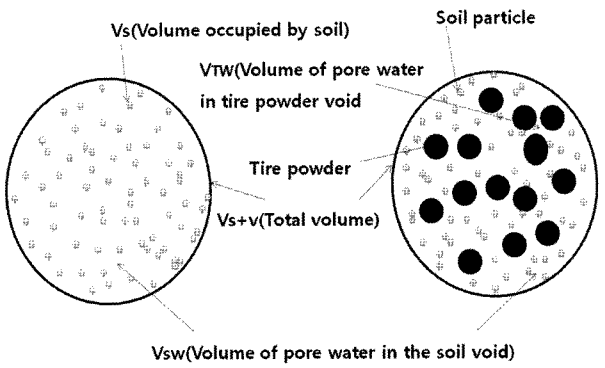

(a) Non-mixed soil (b) Mixed soil

Fig. 10. Cross-sectional states of non-mixed and mixed soils

Table 5. Volume of pore water in soil and tire powder

Mixing ratio (%)	0	5	30	60
V_{SW} (cm^3)	332.0	310.8	231.6	123.8
V_{TW} (cm^3)	–	6.1	25.4	77.5
V_W (cm^3)	332.0	316.9	257.0	201.3
Permeability (cm/sec)	4.03×10^{-6}	6.93×10^{-6}	9.45×10^{-6}	1.15×10^{-5}

Table 5 shows that when the mixing ratio increases from zero to 60 percent, V_{SW} reduces from 332.0 to 123.8 cm^3, while V_{TW} rises from zero to 77.5 cm^3. Although V_W decreases from 332.0 to 201.3 cm^3 with an increase in the mixing ratio, the coefficient of permeability increases gradually. Fig. 11 illustrates the relationship between the mixing ratio and permeable cross section. We think that the powder less than 1 mm in diameter has characteristics similar to sand; therefore, the higher the mixing ratio of tire powder, the larger the permeable cross section at temperatures above zero, resulting in an increase in permeability.

The coefficient of permeability is said to relate to the area of water rather than to the volume of water. We find the permeable cross sections shown in Fig. 11 by applying V_S and V_T derived from the three phases of the soil as well as V_{SW} and V_{TW} shown in Table 5 to Eqs. (4) and (5) shown below to find the water volume, and converting it with Eq. (6).

$$V_{Soil} = V_S + V_{SW} \tag{4}$$

$$V_{Powder} = V_T + V_{TW} \tag{5}$$

$$A_{(Soil,Powder)} = V_{(Soil,Powder)}^{2/3} \tag{6}$$

Where, Vsoil is the volume of the soil component of the sample and Vpowder is the volume of tire powder. As shown in Fig. 11, as the mixing ratio of tire powder increases, the soil area Asoil decreases but the powder area Apowder increases.

At temperatures above zero, Asoil + Apowder shown in Figure 11 is the permeable area. Fig. 12 illustrates the relationship between total permeable area and mixing ratio. At temperatures above zero, the permeable area rises from 71.8 to 90.2 cm^2 with an increase in the mixing ratio (see Fig. 12 +Temperature).

We think that the tire powder has sand-like characteristics and is water-repellent; therefore, it contains no unfrozen water at temperatures below zero. As a result, water included in powder voids is completely changed to ice at temperatures below zero, which is likely to stop the flow of water. In this case, water can flow only through

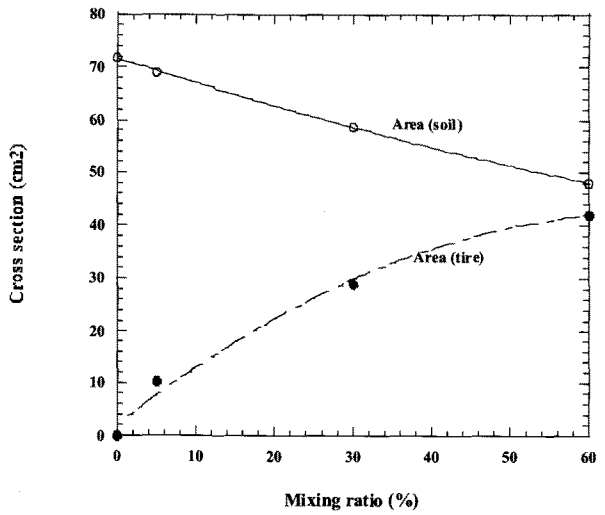

Fig. 11. Variation in mixing ratio and permeable cross section

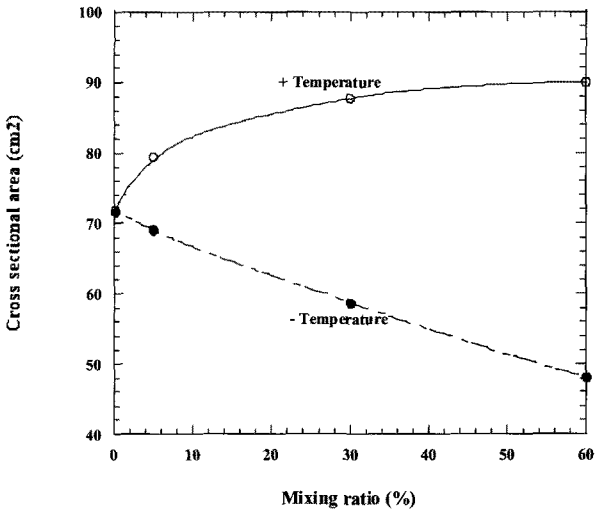

Fig. 12. Permeable area of soil

the soil; therefore, as the mixing ratio increases, the permeable cross-section decreases. The permeable area at temperatures below zero is only Asoil shown in Fig. 11, which tends to be inversely proportional to the mixing ratio. For example, mixing ratios of zero and 60 percent present permeable areas of 71.8 and 48.1 cm^2 respectively (see Fig. 12 -Temperature), which correspond to a reduction of about 43 percent. According to Figs. 11 and 12 showing the relationship between permeable area and mixing ratio, as the mixing ratio increases at temperatures below zero, the permeable area decreases, resulting in a reduction in permeability (see Table 5).

5.2 Variations of Unsaturated Coefficient of Permeability in an Unfrozen State

When the temperature falls below zero, ice is formed in soil voids. This pore ice decreases the water flowing area by the corresponding area. The coefficient of permeability of the frozen fringe where pore ice is present is very difficult to measure. However, we expect that using a method of finding the unsaturated coefficient of permeability at temperatures above zero enables calculation of the coefficient of permeability of the frozen fringe.

According to Black and Tice (1988), if two kinds of cohesive soil have the same density and water content - - the unfrozen water content at low temperatures is the same as the water content in an unsaturated state at the normal temperature - - then the two pore water distributions are consistent with each other as shown in Fig. 13. They compared the unfrozen water content measured with the pulse NMR system and the water retention curve derived from the pF test. Black and Tice claim that the following relation holds between the temperature of a freezing state and the air pressure at normal temperature.

$$\phi_{aw} = \phi_{iw} \tag{7}$$

$$\phi_{aw}(kPa) = -1{,}110(kPa/°C) \times T_S(°C) \tag{8}$$

where, ϕ is the pressure difference (kPa), T_S is the growing temperature of ice lens, and the subscripts a, w, and i represent air, water, and ice, respectively. If the frozen soil temperature is -1 degree Celsius, the sample has a pore ice distribution in the soil, which is equivalent to an air distribution in the pF test at a pressure of 1,110 kPa. This is the modified Clausius-Clapeyron equation.

Fukuda and Tice (1980) show the following experimental equation to represent the unsaturated coefficient of permeability of the same Tomakomai soil as that used in this research as a capillarity potential function:

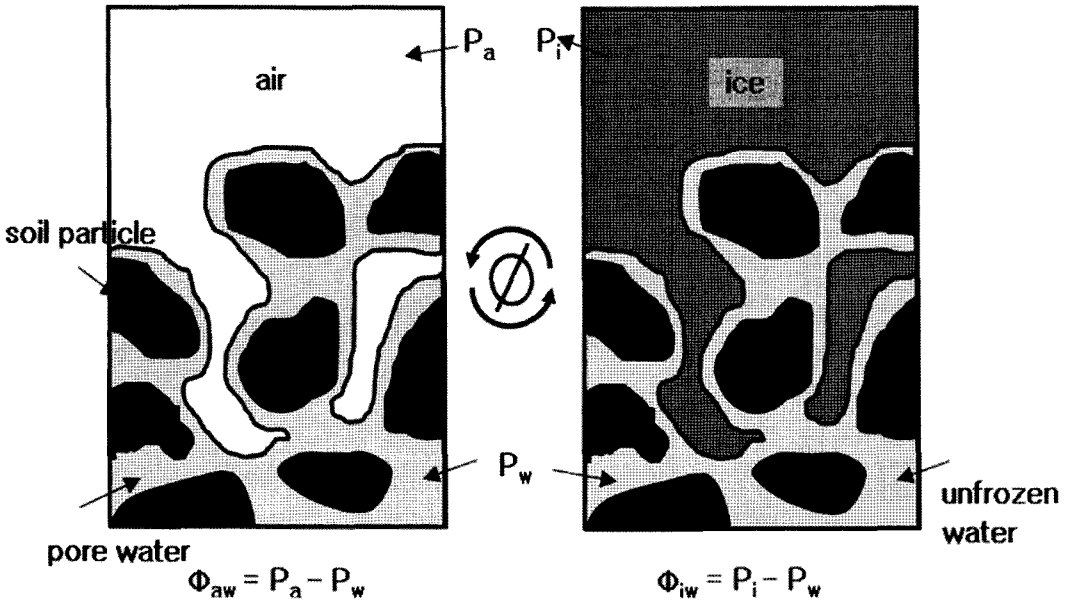

(a) Unsaturated soil at normal temperature (b) Frozen soil

Fig. 13. Distributions of unfrozen and pore water at the same water content (Black and Tice (1988))

$$-\log_{10}(K) = A + B/\phi_{aw} \quad (9)$$

where, K is the unsaturated coefficient of permeability (cm/sec), ϕ is the capillarity potential (pF), and A and B are factors (9.549 and -6.614 respectively).

Substituting equation (8) into equation (9) and converting kPa to g/cm^2 produces equation (10) below.

$$-\log_{10}(K) = 9.549 - 6.614/(-1110 \cdot 10 \cdot Ts) \quad (10)$$

Eq. (10) shows that the relationship between the unsaturated coefficient of permeability and the pF is changed to that between the former and the temperature. Accordingly, we must determine the growing temperature T_S of ice lens. However, we could not measure T_S in this research, so we used Eq. (10) and the temperature range of -0.25 to -1.0 degrees Celsius - - the developing and growing temperatures of ice lens formed in ordinary soil - - to find the unsaturated coefficient of permeability (Masami et al., 2002). Fig. 14 shows the resulting Kuu curve.

5.3 Variations of Unsaturated Coefficient of Permeability in a Frozen State

In the calculation of the unsaturated coefficient of permeability in an unfrozen state in the previous subsection, we assume that air exists instead of ice. When air is present in a void, the friction between the air and water can be ignored, but in the presence of ice instead of air, the resulting resistance between the ice and water lowers the speed of the flow of water. This means that finding the coefficient of permeability of the frozen fringe requires taking the resistance of ice into consideration. According to research conducted by Burt and Williams (1970), the resistance corresponds to 10^{-2} times of an unfrozen permeability coefficient. This is the ice-impeding factor. In this research, we apply the value to the coefficient of permeability (Kuu curve) shown in Fig. 14 to find the unsaturated coefficient of permeability of the frozen fringe (Kuf curve).

5.4 Apparent Unsaturated Coefficient of Permeability of the Mixed Soil

In Subsection 5.1, we mentioned that water was present as free water in the discarded tire powder at temperatures above zero. However, when the temperature fell below zero, pore water was frozen, resulting in no water flow. Accordingly, the coefficient of permeability of the frozen fringe of the mixed soil is derived from changes in the cross sections of the soil and tire powder, which depend on the mixing ratio of the latter as shown in Fig. 11. Fig. 15 indicates changes in the coefficient of permeability when the temperature range is -0.25 to -1.0 degrees Celsius and the mixing ratio is 0, 5, 30, or 60 percent.

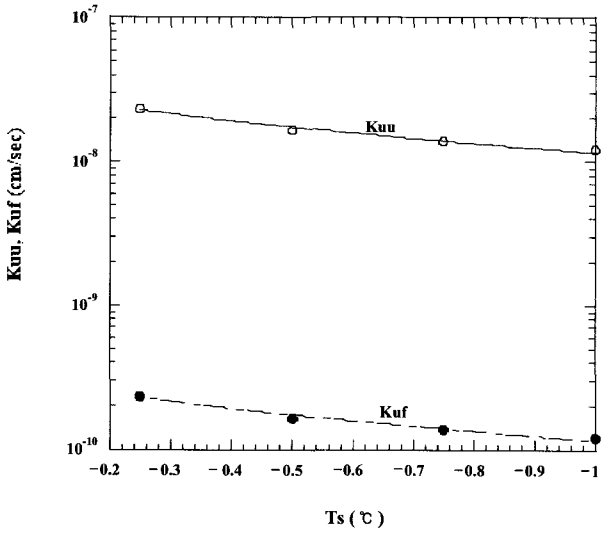

Fig. 14. T_S and unsaturated coefficients of permeability in unfrozen and frozen states

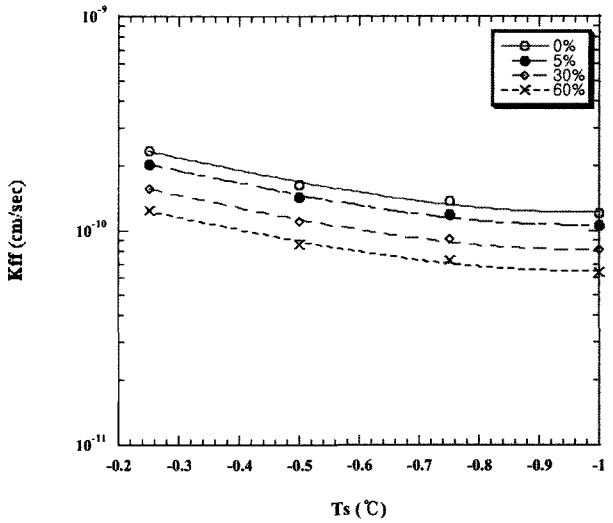

Fig. 15. Unsaturated coefficient of permeability of frozen fringe

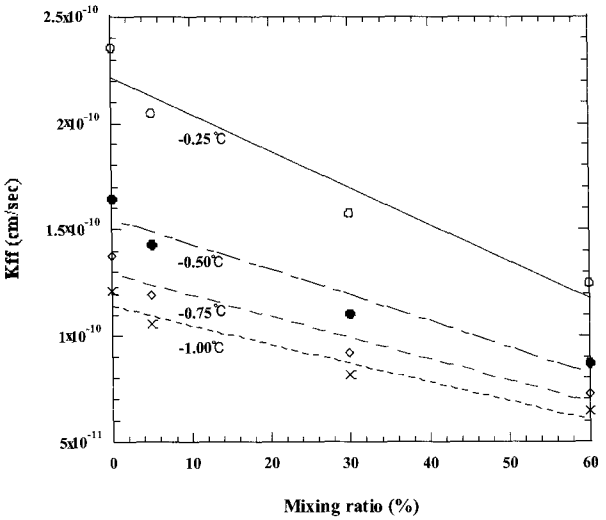

Fig. 16. Unsaturated coefficient of permeability and mixing ratio

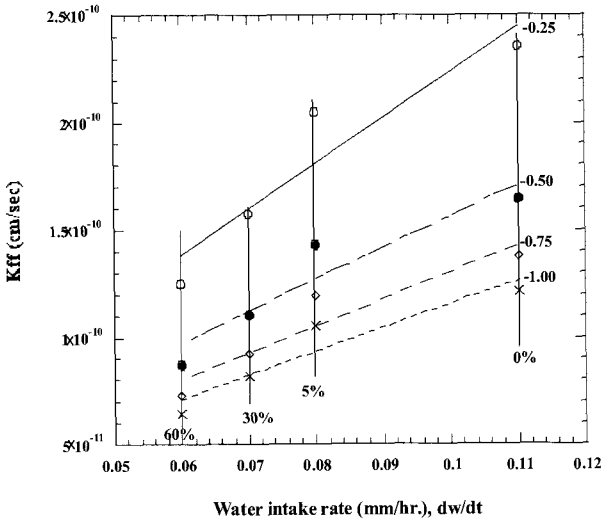

Fig. 17. Relationship between coefficient of permeability and water intake rate

As shown in Fig. 11, the cross sections (permeable areas) of the soil and tire powder are 69 cm^2 and 10.4 cm^2, respectively, if the mixing ratio is, for example, five percent. The soil component accounts for an 87% share of the entire cross section. Multiplying the ratio of the resulting cross section of the soil by Kuf in Fig. 14 on a powder mixing ratio basis yields the coefficient of permeability shown in Fig. 15. As the temperature T_S changes from -0.25 to -1 degrees Celsius, the tire powder mixing ratio increases but the coefficient of permeability decreases.

Fig. 16 shows the relationship between the coefficient of permeability of the mixed soil (Fig. 15) and the mixing ratio with the growing temperature T_S of ice lens parameterized. So long as T_S is within the range of -0.25 to -1 degrees Celsius, increasing the mixing ratio tends to decrease the coefficient of permeability Kff. We think that the reason why a temperature reduction decreases the coefficient of permeability is that the speed of water flowing through the frozen fringe is lowered due to decrease of unfrozen water (Fig. 4).

5.5 Unsaturated Coefficient of Permeability and Water Intake Rate

Fig. 17 shows the relationship between the unsaturated coefficient of permeability (Kff) of the frozen fringe and the water intake rate (dw/dt). The latter is given by dividing the amount of frost heave shown in Fig. 8 by a bulk modulus of 1.09 when water is frozen - - the displacement per unit time.

Water in the tire powder is completely frozen at temperatures below zero, eliminating any water flowing route. Assuming that only the soil component shows a frost heave and the pressure gradient (dpw/dx) of the soil is constant regardless of the mixing ratio, the water intake rate is represented by the following equation including the unsaturated coefficient of permeability:

$$\frac{dw}{dt} = K_{ff} \cdot \frac{dpw}{dx} \qquad (11)$$

If the pressure gradient is constant in Eq. (11), a linear relationship exists between the coefficient of permeability and the water intake rate (see Fig. 17). Fig. 17 indicates that increasing the amount of mixed tire powder reduces the coefficient of permeability, resulting in a fall in the water intake rate.

6. Conclusions

Through field tests, we have confirmed that mixing of tire powder has the effect of suppressing frost heave (Kim et al., 2010). To clarify the mechanism of this effect, we used the same tire powder to conduct three kinds of laboratory experiments: unfrozen water content, thermal

conductivity, and frost heave.

In this research, we focused on changes in the coefficient of permeability caused by mixing of tire powder, and first found it in an unsaturated state. In the presence of ice, we took the ice-impeding factor into consideration to derive the coefficient of permeability of the frozen fringe from the ratio of the soil and tire powder areas in the mixed soil. The results showed that a linear relationship exists between the water intake rate and the coefficient of permeability. Accordingly, we have concluded that the frost heave reduces thanks to a fall in the permeability and a reduction in the unfrozen water content of the soil mixed with tire powder.

In addition, we calculated the volumetric ratio of the soil and tire powder to quantify the moisture amount of soil and tire powder pores. The results show that:

(1) At temperatures above zero, as the mixing ratio of tire powder increases, the water content of tire pores rises from zero (at a mixing ratio of 0 percent) to 77.5 cm^3 (at 60 percent). When the temperature falls below zero, water in the tire powder completely changes to pore ice at zero degrees, eliminating any water passing route. As the tire powder content increases, the unfrozen water in the soil component decreases.

(2) When we take the cross-section ratio into consideration and increase the mixing ratio of tire powder from zero to 60 percent, the coefficient of permeability of the frozen fringe decreases; for example, from 1.64 $\times 10^{-10}$ to 8.71 $\times 10^{-11}$ cm/sec at a temperature of -0.5 degrees Celsius.

(3) The temperature range in which a frozen fringe is present may be from -0.25 to -1.0 degrees Celsius, at which a linear relationship exists between the coefficient of permeability and the water intake rate.

References

1. Black, P.B. and Tice, A.R. (1988), "Comparison of soil freezing curve and soil water curve data for Windsor sandy roam", *CRREL Report 88-16*, pp.1-9.
2. Burt, T.P. and Williams, P.J. (1970), "Hydraulic conductivity in frozen soil", *Earth Surface Processes 1*, pp.349-360.
3. Eaton, R. A., Robert, R. J. and Humphrey, D. N. (1994), "Gravel road sections insulated with scrap tire chip", *CRREL Special Report 94-21*, pp.1-43.
4. Fukuda, M. and Luthin, J.N. (1980), "Pore-water pressure profile of a freezing soil", *Frost I Jord NR. 21*, pp.31-36.
5. Humphrey, D. N., Chen, L. H. and Eaton, R. A. (1997), "Laboratory and field measurement of the thermal conductivity of tire chips for used surged insulation", *Transportation Research Board 76rh annual meeting*, pp.1-27, pp.33-85.
6. Ifukube, M. (1962), "Studies on frost heave, frost penetration and ratio of replacement to prevent frost damage of roads in Hokkaido", *Report of the civil engineering research institute, No. 74.*
7. Ishizaki, T. (1994), "Temperature dependence of unfrozen water film thickness in frozen soils", *Snow and Ice*, Volume 56, No. 1, pp.3-9.
8. Kim, H.S., Suzuki, T., Fukuda, M., Seo, S.Y., and Yamashita, S. (2010), "Field experiments for reducing frost susceptibility using recycled tire powder", *Journal of the Korean geotechnical society*, (in press).
9. Kinosita, S. (1979), "Effects of initial soil-water conditions on frost heaving characteristics", *Engineering Geology*, 13, pp.41-52.
10. Zimmer, J. (1996), "Scrap tire recovery: An analysis of alternative", *Texas Scrap Tire Market Development Conference, Texas Natural Resource Conservation Commission*, pp.63-76.

(접수일자 2010. 2. 19, 심사완료일 2010. 4. 24)